OPEN ACCESS

ARTICLE

The Innovation Geoscience

Strong reprocessing of dissolved organic matter along South-to-North water diversion

Xiaofeng Cao,[1,3,4,5,*] Jie Wang,[2,5,*] Zitong Sun,[1] Jianghao Ji,[2] Jiangyong Chu,[1] Yuewei Wang,[1] Weixiao Qi,[1] Jianfeng Peng,[1] Huijuan Liu,[1] and Jiuhui Qu[1]

*Correspondence: xfcao@tsinghua.edu.cn (X.C.); jiewangcau@cau.edu.cn (J.W.)

Received: August 17, 2024; Accepted: November 2, 2025; Published Online: November 8, 2025; https://doi.org/10.59717/j.xinn-geo.2025.100170

GRAPHICAL ABSTRACT

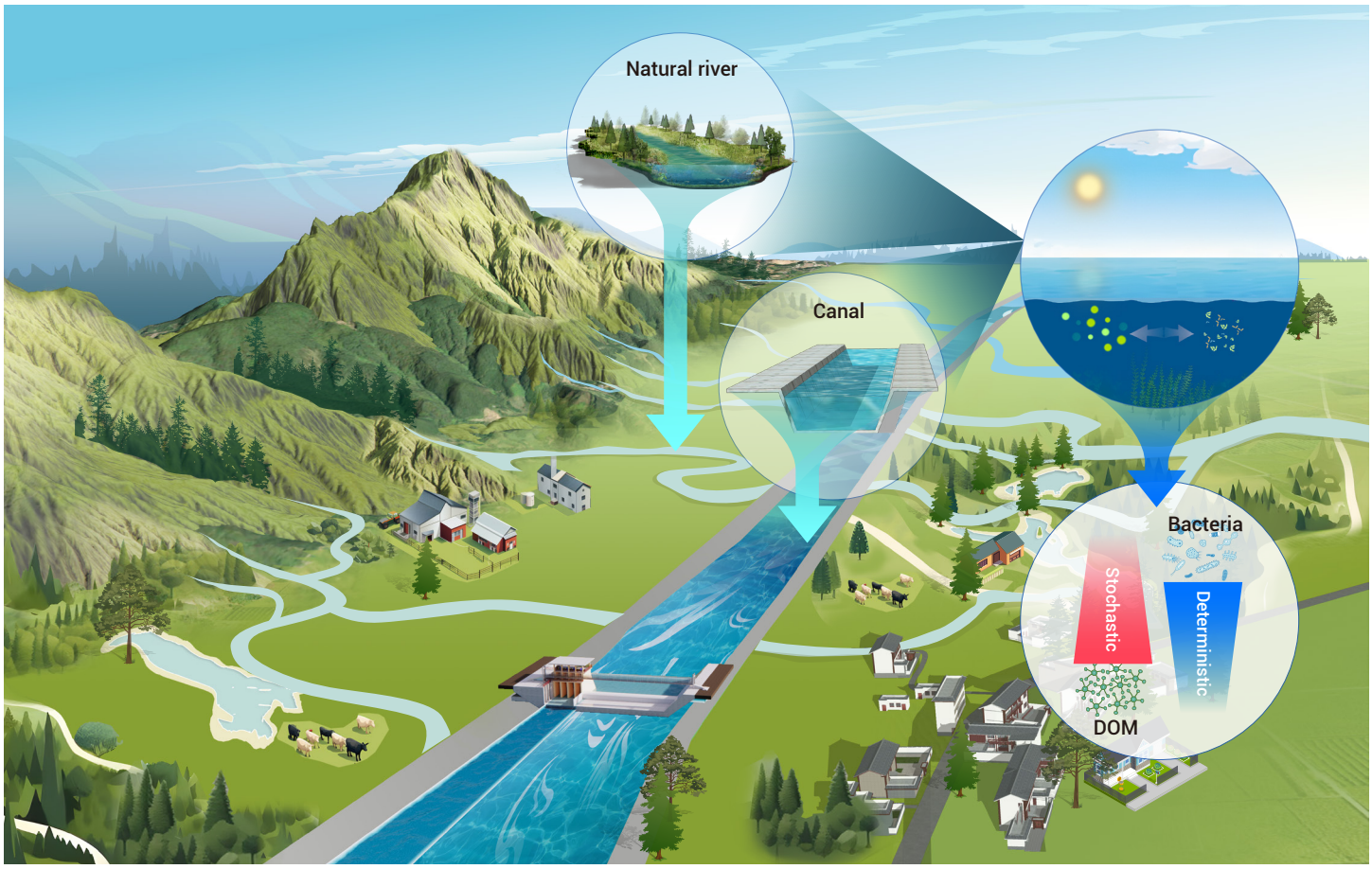

PUBLIC SUMMARY

- Canal waters accumulated more oxidized and recalcitrant DOM formulae.
- DOM composition and bacterial communities showed homogenization in canal waters.
- Microbial transformation drives canal DOM toward homogeneous and recalcitrant characteristics.

ARTICLE

OPEN ACCESS

www.the-innovation.org/geoscience

Strong reprocessing of dissolved organic matter along South-to-North water diversion

Xiaofeng Cao,[1,3,4,5,*] Jie Wang,[2,5,*] Zitong Sun,[1] Jianghao Ji,[2] Jiangyong Chu,[1] Yuewei Wang,[1] Weixiao Qi,[1] Jianfeng Peng,[1] Huijuan Liu,[1] and Jiuhui Qu[1]

[1]Center for Water and Ecology, State Key Joint Laboratory of Environment Simulation and Pollution Control, School of Environment, Tsinghua University, Beijing 100084, China

[2]Beijing Key Laboratory of Farmland Soil Pollution Prevention and Remediation, College of Resources and Environmental Sciences, China Agricultural University, Beijing 100193, China

[3]Center for Ecological Civilization, Tsinghua University, Beijing 100084, China

[4]Center of Tsinghua Think Tanks, Tsinghua University, Beijing 100084, China

[5]These authors contributed equally

*Correspondence: xfcao@tsinghua.edu.cn (X.C.); jiewangcau@cau.edu.cn (J.W.)

Received: August 17, 2024; Accepted: November 2, 2025; Published Online: November 8, 2025; https://doi.org/10.59717/j.xinn-geo.2025.100170

Citation: Cao X., Wang J., Sun Z., et al. (2025). Strong reprocessing of dissolved organic matter along South-to-North water diversion. *The Innovation Geoscience* **3**:100170.

Freshwater ecosystems contain a diverse mix of dissolved organic matter (DOM) molecules, which play a significant role in the global carbon cycle. Here, we discovered an absorbing pattern of DOM-microbe interactions along the Middle Route of the South-to-North Water Diversion Canal in China, the largest water transfer project in the world. Using ultrahigh-resolution mass spectrometry, we tracked the molecular composition of DOM along the canal and analyzed its relationship with planktonic bacterial communities and physicochemical conditions. More oxidized and recalcitrant DOM formulae were accumulated in the canal waters, inducing the enrichment of oligotrophic taxa. Homogenization of DOM composition and bacterial communities was observed in the canal waters. Additionally, negative interactions between DOM molecules and bacterial taxa were more abundant in the canal waters (69.5%) than those in natural waters (32.2%). These results together suggest that the semi-enclosed nature of the canal and the sustained microbial and photochemical transformations drive DOM toward more homogeneity and recalcitrance, necessitating systematic quantification of carbon emissions specific to the South-to-North Water Diversion project. Incorporating carbon reduction strategies and technologies into the design and management of the national water network is scientifically imperative.

INTRODUCTION

Dissolved organic matter (DOM) is a fundamental component of aquatic ecosystems, representing a substantial active carbon reservoirs.[1-3] This complex mixture of over 100,000 distinct molecules plays a pivotal role in aquatic carbon dynamics and energy flow, influencing trophic transfer, greenhouse gas emissions, and water quality.[4-6] Microbial activity is a key driver of DOM transformation, with microbial consortia modulating its molecular composition through the breakdown of larger molecules and the synthesis of recalcitrant compounds from labile substrates.[3,7,8] Furthermore, DOM serves as a vital metabolic substrate, shaping the diversity, structure, and function of microbial communities.[9,10] Understanding the intricate mechanism of DOM-microbe interactions in aquatic ecosystems is therefore crucial for comprehending global carbon cycling and climate regulation, particularly in systems impacted by anthropogenic activities.[11,12]

Anthropogenic activities, including damming,[13] water diversion,[14,15] agricultural activities,[16] and groundwater extraction/recharge,[17] significantly alter DOM properties. For instance, groundwater extraction can release photolabile and aerobically biolabile DOM into surface waters,[17,18] while reservoir impoundment can lead to the selective loss of aromatic organic matter and enrichment of aliphatic DOM.[19] To alleviate water scarcity in major urban centers, large-scale engineering projects, such as interbasin water transfer or water diversion, are implemented to transport water from more humid regions to arid regions (e.g., California and Arizona).[20,21] These projects are integral to national water network development, aimed to safeguarding national water security, but can also have unintended consequences for natural biogeochemical cycles. Among these, China's South-to-North Water Diversion (SNWD) project, designed to transport approximately 45 billion m^3 of water annually from the Yangtze River through three canal and pipeline systems (eastern, middle, and western), stands as the world's largest interbasin water transfer scheme and a crucial component of China nation's "Four Horizontal and Three Vertical" water network framework.[22] However, the impacts of the SNWD, particularly the Middle Route, on canal water DOM properties and the differences between canal and natural water DOM remain poorly understood.

The Middle Route of the SNWD spanns 1,432 km, with approximately 83.5% of its length contructed as an unshaded, concrete-lined open canal.This highly engineered system presents a unique and underexplored artificial aquatic environment. The absence of shading may enhance DOM photo-mineralization to carbon dioxide (CO_2).[23] Furthermore, the canal's semi-enclosed hydraulic design, characterized by limited exchange with surrounding surface, terrestrial environments, and groundwater, results in distinct water residence times and potentially complex biotic and abiotic interactions. These conditions may profoundly influence microbial respiration of DOM and ultimately impact water quality within the system. In this study, we analyzed DOC concentration and DOM molecular composition, alongside water chemistry and microbial community structure, along the Middel Route to elucidate the mechanisms of DOM-microbe association. Simultaneously, we also collected corresponding natural water samples from rivers near the canal at matching latitudes for comparison. We hypothesize that the semi-enclosed concreted channel of the canal would promote the accumulation of more recalcitrant DOM due to the sustained microbial and photochemical transformations, and that the river continuum along the canal would lead to different DOM-microbe interactions compared to natural rivers. These insights aim to provide strategic recommendations for optimizing and enhancing the sustainable development of national water network project, particular concerning long-term water quality and ecosystem health.

MATERIALS AND METHODS

Study sites and sampling collection

To evaluate the effects of the South-to-North Water Diversion (SNWD) Middle Route on dissolved organic matter (DOM) composition and microbial communities, we collected water samples from 20 sites along the canal, spanning its entire course from the Danjiangkou Reservoir to the North China Plain and encompassing both subtropical and warm-temperate climatic zones. For comparison, 20 additional samples were collected from nearby natural rivers located at approximately matching latitudes (with comparable climatic conditions), serving as references for background riverine conditions unaffected by canal water inputs (Figure 1). Surface water samples (0-20 cm depth) were collected in triplicate at each site and combined to create a composite sample. This surface layer was chosen as it represents the photic zone where significant photochemical and biological DOM transformation are likely to occur. Sampling was conducted from March to April in 2023. This period was selected to capture representative conditions during the typical dry season before the onset of significant summer rainfall and associated runoff, which would introduce substantial variability in water quality and DOM characteriatsics.

Prior to water collection, in-situ measurements of physiochemical variables, including temperature, pH, electrical conductivity (EC), dissolved oxygen (DO), and oxidation-reduction potential (ORP), were obtained using a multi-parameter instrument (ProQuatro 606950, YSI incorporated, USA). For subsequent chemical analyses, 1 L water samples were filtered through precombusted (450°C, 4 hours) 0.45 μm (pore size) microporous glass fiber

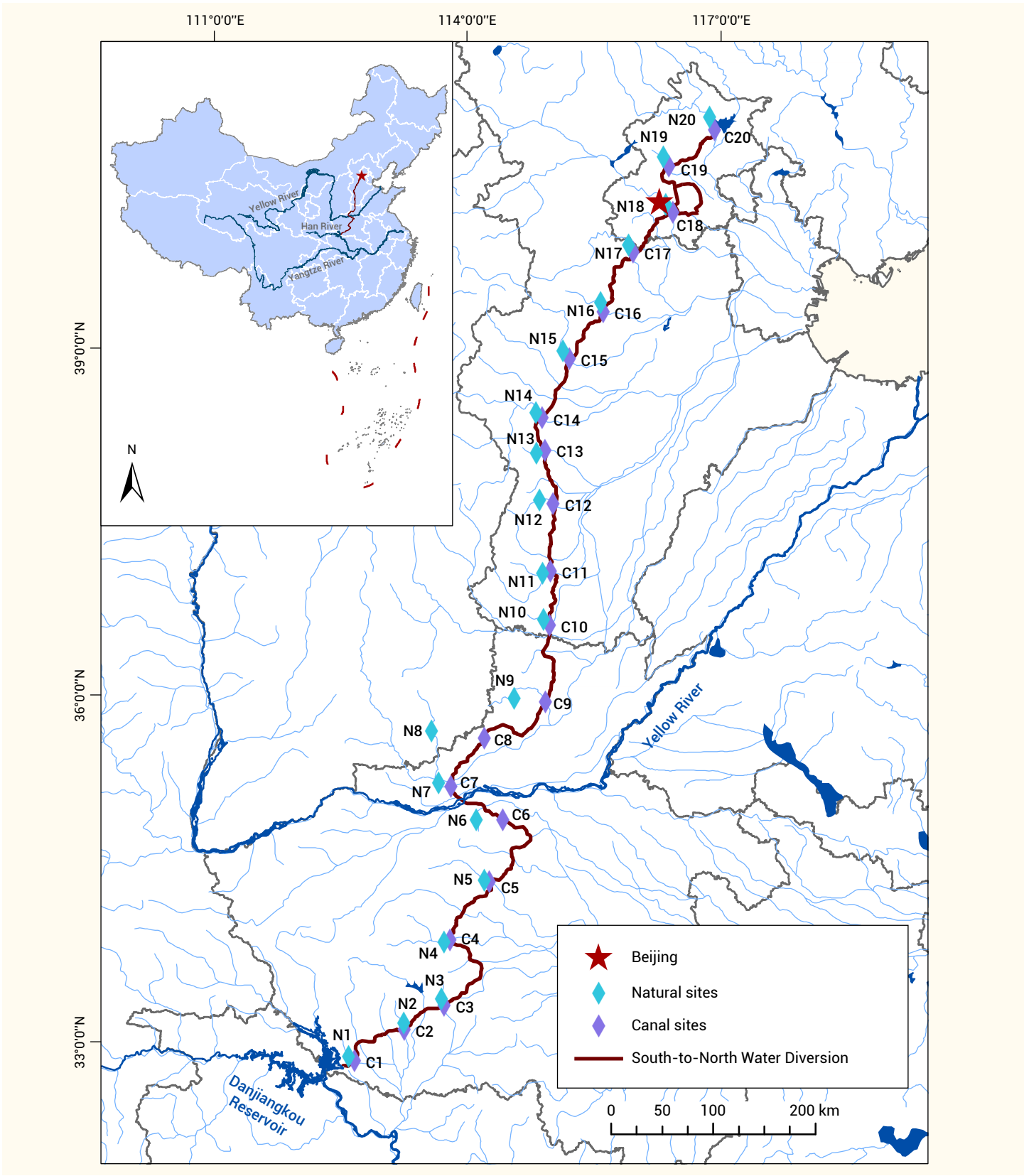

Figure 1. Map of the sampling sites Purple diamonds are the canal water samples, and green diamonds are the natural water samples.

membrane filters into acid-washed amber glass bottles. Chemical analyses included chemical oxygen demand (COD_{Mn}), total nitrogen (TN), total phosphorus (TP), ammonia nitrogen (NH_4^+-N), nitrate nitrogen (NO_3^--N), and dissolved organic carbon (DOC). Detailed results of these analyses are provided in the Supplemental Information (Figure S1).

DOM molecular characteristics

We used Fourier-transform ion cyclotron resonance mass spectrometry (FT-ICR-MS) to explore the molecular composition of DOM in canal and natural water.[24,25] Briefly, water samples were filtered through pre-combusted (450°C, 4 hours) 0.45 μm (pore size) microporous glass fiber membrane

filters and acidified with hydrochloric acid (1 mol/L) to pH 2. Solid-phase extraction (SPE) was performed using a reversed-phase BondElut PPL cartridge (500 mg, 6 mL, Agilent Technologies). Briefly, cartridges were activated with 6 mL methanol (HPLC grade) and loaded with water samples by gravity at approximately 1 mL/min. The cartridges were then rinsed with 18 mL of acidified deionized water (pH = 2) and dried under N_2 gas. DOM was then eluted with 12 mL of methanol, concentrated to near dryness with N_2 gas, and reconstituted in 1.0 mL of methanol in a GC vial.[26,27] DOM samples were measured with a Bruker SolariX FT-ICR-MS with a 15.0 T superconducting magnet with an ESI ion source in negative ion mode. The ESI needle voltage was set to -3.8 kV. Two hundred scans with 8 M words of data were collected per sample, resulting in a mass resolving power greater than 1,000,000 (at m/z 400). The lower and upper mass limits were set to mass-to-charge (m/z) values of 100 and 800, respectively. Raw spectra were converted to a list of m/z values using DataAnalysis software 4.2 (Bruker Daltonik GmbH, Bremen, Germany) with a signal-to-noise of > 4 and a default intensity threshold of 100. Putative chemical formulas were assigned using software from the Environmental Molecular Sciences Laboratory based on the compound identification algorithm,[28] described by Kujawinki and Behn.[29] The mass error for a given chemical formula was set to < 0.35 ppm. DOM formulas were categorized to seven groups based on oxygen-to-carbon (O/C) and hydrogen-to-carbon (H/C) ratios: lipid-like (O/C, 0-0.3; H/C, 1.5-2.0), protein/amino sugar-like (O/C, 0.3-0.37; H/C, 1.5-2.2), carbohydrate-like (O/C, 0.67-1.2; H/C, 1.5-2.2), highly unsaturated and phenolic-like (O/C, 0-0.1; H/C, 0.7-1), lignin-like (O/C, 0.1-0.67; H/C, 0.7-1.5), tannin-like (O/C, 0.67-1.2; H/C, 0.5-1.5), and condensed aromatic-like (O/C, 0-0.67; H/C, 0.2-0.7) compounds. The double bond equivalence (DBE), the nominal oxidation state of carbon (NOSC), the Gibbs free energy for the half-reaction of carbon oxidation (ΔG), and the modified aromaticity index (AI) of each formula were calculated as follows:

$$DBE = 1 + \frac{1}{2}(2C - H + N) \quad (1)$$

$$NOSC = 4 - \frac{4C + H - 3N - 2O - 2S}{C} \quad (2)$$

$$\Delta G = 60.3 - 28.5 \times \mathrm{NOSC} \quad (3)$$

$$\mathrm{AI} = \frac{1 + \mathrm{C\text{-}0.5C\text{-}S\text{-}0.5}H}{\mathrm{C\text{-}0.5O\text{-}S\text{-}N}} \quad (4)$$

where C, H, O, N, and S refer to the number of atoms per formula of carbon, hydrogen, nitrogen, oxygen, and sulfur, respectively. Additionally, the percentage of labile-like compounds (molecular lability boundary, MLB) was calculated by the number of molecules with H/C ≥ 1.5 divided by the total molecular number in the sample.[30,31] The carbon use efficiency (Y_{met}), which refers to the thermodynamic efficiency of metabolic reactions involved in biomass production,[32] was calculated following the R code supplied by Hu et al.[33] Weighted means of formula-based molecular traits were calculated as the sum of the product of the trait value for each individual molecule and relative intensity divided by the sum of all intensities.[33] Furthermore, we calculated the potential biochemical transformations between molecules within each sample based on the mass differences between FT-ICR-MS peaks.[34] All possible pairwise mass differences were assigned to specific compounds in a transformation database (https://github.com/danczakre/Meta-Metabolome_Ecology). The energy changes involved in the molecule transformations (ΔG) are defined as the differences in the Gibbs free energy of the molecule before and after the transformation.[35] The transformation with ΔG ≤ 0 could happen spontaneously in thermodynamics and be a thermodynamically favorable process (TFP), while the transformation with ΔG > 0 requires external energy and could be treated as a thermodynamically limited process (TLP).

Microbial community composition

Approximately 1 L of water sample was filtered through a 0.22 μm filter (Sterivex GP 0.22, Millipore), and the filter was used to extract microbial DNA using the PowerWater DNA Isolation Kit (Qiagen, Shanghai, China). DNA quality and concentration were assessed using a NanoDrop Spectrophotometer (ND-2000, Thermo Scientific, Wilmington, DE, US). The V3-V4 region of the 16S rRNA gene was amplified by the primers 338F (ACTCCTACGGGAGGCAGCA) and 806R (GGACTACHVGGGTWTCTAAT). The details of the polymerase chain reaction are provided in Supplementary Information. Amplicons were purified and sequenced on the Illumina Miseq platform with 2 × 300-bp paired-end format at Majorbio BioPharm Technology Co. Ltd (Shanghai, China).

Quantitative Insights Into Microbial Ecology 2 (QIIME2, version 2020.2) with the DADA2 plugin was used to process raw reads.[36] After checking the quality of the acquired raw data, the barcodes and primers were cut. We further trimmed the forward sequences to 280 base pairs and the reverse sequences to 200 base pairs. The sequences were merged, denoised, and clustered into amplicon sequence variants (ASVs). The SILVA reference database (version 132) was used to assign the taxonomic information of each representative ASV.[37]

Statistical analysis

Relative intensities of molecules and relative abundance of microbial ASVs were used for the analyses of DOM and microbial characteristics. Bray-Curtis dissimilarities were used to assess the difference between canal and natural samples, and the results were visualized by principal coordinates analysis (PCoA) using the vegan R package. One multivariate analysis of variance (analysis of similarity [ANOSIM]) was used to test the significance of differences between canal and natural water using the vegan R package. To evaluate the composition differences among canal and natural water across all sampling sites, we calculated two values: the pairwise dissimilarity among communities and the dispersion within each group (the multivariate distances between individual samples and the sample centroids).[38,39]

We quantified the relative importance of stochastic versus deterministic processes for the assembly of DOM molecules in canal and natural water via a dendrogram-based ecological modeling approach.[33,40,41] Briefly, we first built a molecular dendrogram from 13 functional trains of DOM molecules. The potential molecular similarities between chemical formulae were calculated to perform a UPGMA hierarchical cluster analysis using the "average" method with the function "hclust" in the stats R package. The beta mean nearest taxon distance metric (βMNTD) was calculated to quantify the molecule dendrogram-based turnover, which estimates the mean dendrogram distance to the closest relative in a paired assemblage for all molecules. We then calculated the dendrogram-based beta nearest taxon index (βNTI), which compares the observed βMNTD and the null distribution of βMNTD. For this calculation, 999 randomized null assemblages were generated by shuffling the tips of the dendrogram. A value of |βNTI| > 2 suggests that the observed molecular assemblage differences are primarily governed by deterministic processes, which can be divided into homogeneous (βNTI < -2) and heterogeneous (βNTI > 2) selection. Stochastic processes are responsible if a value of |βNTI| is less than 2. We further distinguished stochastic processes by using the identity-based Raup-Crick (RC). Null communities were probabilistically generated using 999 iterations per pairwise comparison based on observed molecular assemblages. The null distribution of the Bray-Curis dissimilarity values was compared to the observed value to calculate the deviation from the null expectation, termed as RCbray. A value of |RCbray| > 0.95 represents homogenizing dispersal (RCbray < -0.95) or dispersal limitation (RCbray > 0.95). If a value of |RCbray| < 0.95, the molecular assemblages were as different as would be expected by random chance.

A null model-based analysis of phylogenetic beta diversity was used to estimate the potential contribution of different community assembly processes.[42,43] For each pair of communities, if the phylogenetic-based βNTI > 2, the community turnover was dominantly governed by heterogeneous selection. If βNTI < -2, homogeneous selection was the primary assembly process. If a value of |βNTI| ≤ 2 and the taxonomic dissimilarity (Bray-Curtis) was significantly higher (the modified Raup-Crick metric based on Bray-Curtis dissimilarity, RCbray > 0.95) or lower (RCbray < -0.95) than the null model expectation, the community turnover would be controlled by dispersal limitation or homogenizing dispersal, respectively. If a value of |βNTI| ≤ 2 and a value of |RCbray| ≤ 0.95, the community turnover was regarded as governed by stochastic drift, diversification, weak selection, and dispersal, named 'drift' for short. These analyses were performed using the

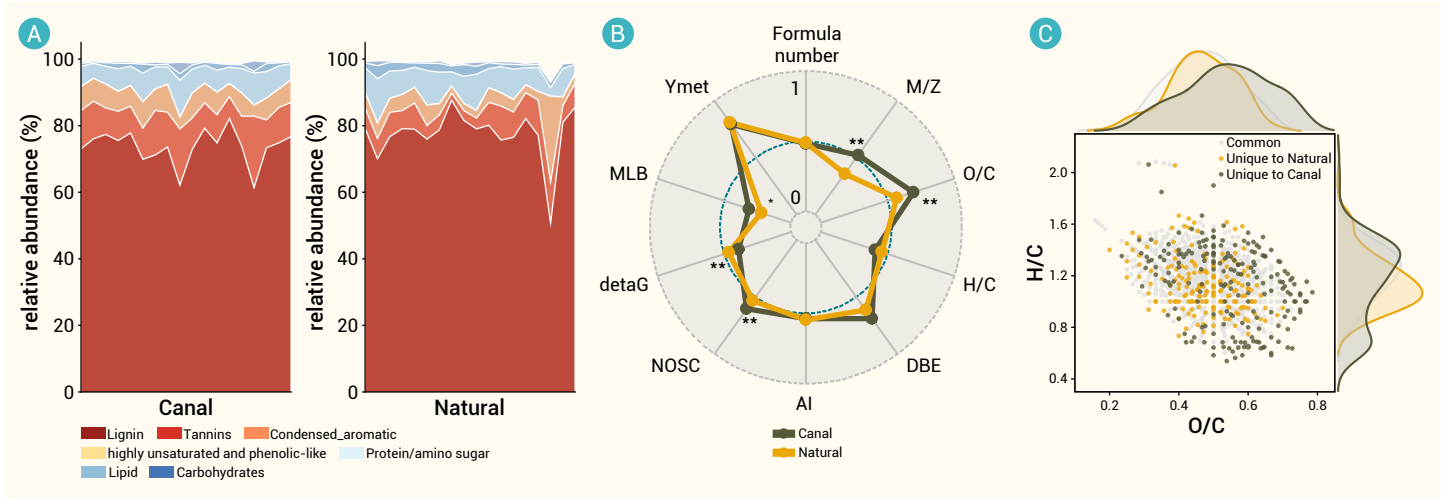

Figure 2. Characteristics of dissolved organic matter (DOM) in natural and canal waters (A) The relative abundance of the seven subcategories in natural and canal waters (condensed aromatic-like compounds, carbohydrate-like compounds, lignin-like compounds, lipid-like compounds, protein/amino sugar-like compounds, tannin-like compounds, unsaturated hydrocarbon-like compounds). (B) The molecular traits of natural and canal DOM (M/Z, molecular mass; O/C, the ratio of O number to C number; H/C, the ratio of H number to C number; DBE, double bond equivalents; AI, aromaticity index; NOSC, nominal oxidation state of carbon; detaG, standard Gibb's free energy of carbon oxidation; Y_{met}, carbon use efficiency; MLB, the number of molecules with H/C ≥ 1.5 divided by the total molecular number). (C) van Krevelen Diagram (VKD) with marginal density plots of molecular formulae. VKD shows formulae unique to only natural waters or canal waters, and molecular formulae common to all samples. Statistical significance is based on Kruskal-Wallis rank-sun tests; * $p < 0.05$, ** $p < 0.01$, *** $p < 0.001$.

iCAMP R package.

To assess the relationship between variation in water physiochemical variables and variation in DOM composition or microbial communities, we first used Procrustes analysis and Mantel tests.[44] Furthermore, a partial Mantel test was used to assess the relationship between each environmental variable and DOM composition or microbial communities.[45] Statistical significance was determined using 999 permutations. These analyses were performed using the vegan R package. We further quantified the associations between DOM molecules and microbial ASVs using the co-occurrence analyses following previous studies.[8,33,46] Briefly, Spearman's rank correlation coefficient ρ between the relative abundance of each molecule and bacterial ASV was calculated using the stats R package. For each DOM molecule, we calculated the Spearman ρ difference (Δρ) by subtracting the mean absolute coefficient value of all the negative correlations with individual bacterial ASVs from the mean of the positive correlations. Positive and negative Δρ values suggest a more strongly positive and negative correlation between DOM molecules and bacterial ASVs, respectively. We visualized the Δρ values against the molecular H/C and O/C. In addition, we estimated the molecule-ASV bipartite networks using SparCC (Sparse Correlations for Compositional Data) method using the SpiecEasi R package.[47] To ensure the reliability of correlation calculation, a threshold of |ρ| = 0.40 was chosen to exclude weak interactions. Negative and positive sub-networks were obtained on the basis of negative and positive correlation coefficients (SparCC ρ < -0.40 or SparCC ρ > 0.40). According to the resource-consumer relationship, negative interactions likely indicate the degradation of larger molecules into smaller structures, while positive interactions may suggest the production of new molecules via degradation or biosynthetic processes.

RESULTS

Homogenization of DOM and microbe in canal

Fourier-transform ion cyclotron resonance mass spectrometry identified 13,649 unique molecular formulas in the canal and natural waters. Lignin-like compounds were the most abundant in both systems, comprising for 83.2% and 81.9% of molecular formulae in the canal and natural waters, respectively (Figure 2A). Tannins-like and protein/amino sugar-like compounds were also prevalent, with significantly higher percentages of tannin-like compounds observed in canal water. The mean ± standard deviation values for percentages of tannin-like compounds in canal and natural water were 10.5 ± 3.5% and 6.3 ± 2.7%, respectively.

In parallel, canal DOM exhibited greater recalcitrance compared to natural DOM, as evidenced by higher values of M/Z, O/C, NOSC, and lower values of ΔG (Figure 2B). Higher M/Z generally indicates larger molecules, while higher O/C and NOSC suggests a greater degree of oxidation. For instance, the mean ± standard deviation of O/C was 0.505 ± 0.023 in canal water, which was significantly ($p < 0.05$) higher than that in natural water (0.467 ± 0.012). Additionally, as shown by the van Krevelen Diagram in Figure 2C, the DOM molecular formulae of canal and natural waters were highly divergent. More recalcitrant-like compounds with higher O/C and lower H/C values were in canal DOM, whereas natural DOM was dominated by smaller, more bioavailable compounds. Consistent with this, thermodynamic spontaneity analysis revealed a significantly higher percentage of thermodynamically favorable processes (TFP) in natural waters compared to canal waters (Figure S2), suggesting more recalcitrant and lower transformability of canal DOM.

We further visualized the differentiation between canal and natural DOM using PCoA based on Bray-Curtis dissimilarity and found that canal DOM was generally separated from the natural DOM (Figure 3A). The ANOSIM results further indicated the separation between the canal and natural DOM was significant ($R = 0.1765$, $p = 0.001$). Simultaneously, canal DOM exhibited greater homogeneity, with lower within-group dissimilarity and distance to centroid compared to natural DOM (Figures 3B-C).

Analysis of 16S rRNA gene sequences yielded 4,032,142 sequences, which were clustered into 12231 amplicon sequence variants (ASVs). Bacterial richness, diversity, and evenness did not differ significantly between natural and canal waters (Figure 4). However, significant differences in community composition were observed. Natural waters were dominated by Proteobacteria (53.1%), Firmicutes (23.1%), and Bacteroidota (15.0%), which were significantly ($p < 0.05$) more abundant than those in the canal waters (35.3%, 18.6%, and 5.10%, respectively). The relative abundances of the phylum Actinobacteriota (31.7%), Cyanobacteria (5.12%), and Verrucomicrobiota (3.94%) were significantly higher in canal waters. At the class level, the relative abundances of Gammaproteobacteria (47.2%) and Bacteroidia (15.0%) in the natural waters were higher than those in the canal waters (29.9% and 5.08%, respectively), whereas other dominant classes, including Actinobacteria, Acidimicrobiia, Cyanobacteriia, Verrucomicrobiae, and Deinococci, were more prevalent in the canal waters. These shifts in microbial composition, with an increase in Actinobacteriota known for their metabolic versatility, may reflect an adaptation to the altered DOM characteristics in the canal. PCoA analysis of bacterial ASVs revealed significant clustering based on water source (Figure 3D), with an ANOSIM R value of 0.5977 ($p = 0.001$). Similar to DOM, bacterial communities in canal waters exhibited greater homogeneity compared to natural waters (Figures 3E-F).

Mechanisms underlying DOM and microbial assembly

To estimate the mechanisms shaping DOM composition and microbial

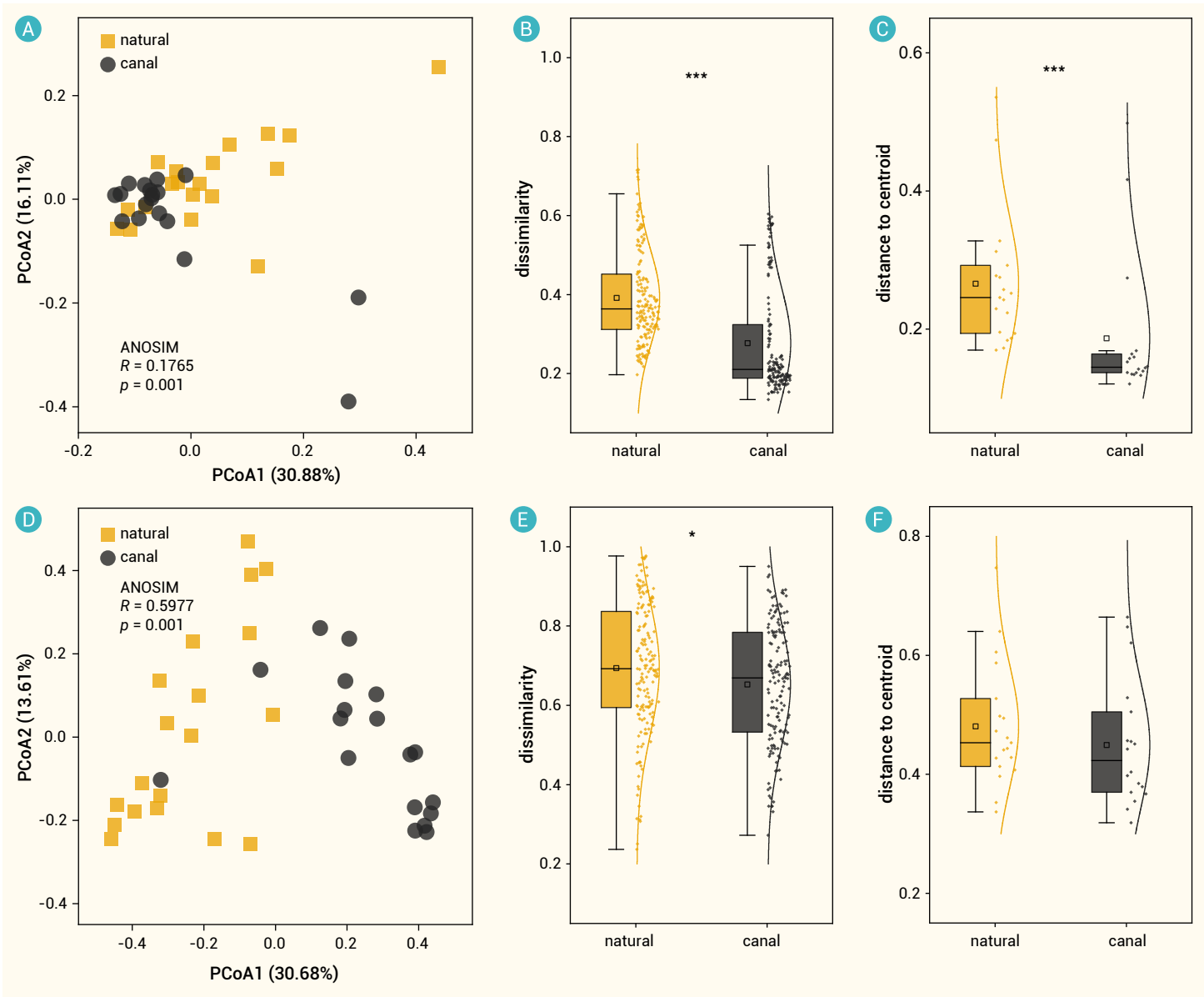

Figure 3. Homogenization of DOM and bacterial communities in canal waters (A) PCoA on the basis of Bray-Curtis distance revealing the dissimilarity of DOM between canal and natural waters; (B) The within-group (canal or natural waters) DOM dissimilarity on the basis of Bray-Curtis distance; (C) The DOM heterogeneity (the distances to the group centroid derived from betadisper function) in natural and canal waters. (D) PCoA on the basis of Bray-Curtis distance revealing the dissimilarity of bacterial communities between canal and natural waters; (E) The within-group (canal or natural waters) dissimilarity of bacterial communities on the basis of Bray-Curtis distance; (F) The heterogeneity of bacterial communities (the distances to the group centroid derived from betadisper function) in natural and canal waters. Statistical significance is based on Kruskal-Wallis rank-sun tests; * $p < 0.05$, ** $p < 0.01$, *** $p < 0.001$.

communities, Procrustes analysis and Mantel test were carried out among the environmental variables, DOM molecules, and microbial communities (Figure S3). The results revealed a significant correlation between environmental variables and microbial communities, with the Procrustes sum of squares $M^2 = 0.7911$ ($p = 0.001$) and Mantel correlation coefficient $R = 0.2286$ ($p = 0.001$). However, the associations between DOM composition and environmental variables, as well as those between DOM and microbial community, were not significant. Partial Mantel test further suggested a stronger influence of environmental variables on microbial communities than on DOM (Figure 5A). Microbial community dissimilarity increased with geographic distance, indicating a distance-decay pattern potentially driven by spatial constraints on dispersal, whereas no clear distance-decay pattern was observed for DOM (Figures 5B-C). Furthermore, environmental variables exerted a stronger influence in nature waters. In canal waters, DOM composition was primarily related to DOC concentration, and microbial community to longitude (Figure S4). In natural waters, TP strongly correlated with DOM, and longitude, latitude, EC, ORP, and the inorganic nitrogen with microbial communities (Figure S4), highlighting the influence of a range of physico-chemical factors in natural systems.

Null model analysis revealed distinct assembly mechanisms for microbial communities and DOM (Figure 6). For the microbial community, the βNTI values were < 2 across all water samples, suggesting the negligible contribution of heterogeneous selection (HeS) for the microbial assembly (Figure 6A). The deterministic homogeneous selection (HoS) accounted for 46.8% of the patterns of compositional structure across natural waters and 67.9% across canal waters (Figures 6B-C), potentially implying that similar environmental filtering pressures play a significant role in shaping microbial communities. The stochastic dispersal limitation (DL) and Drift (DF) also contributed to the microbial assembly, with 24.7% and 24.1% in natural waters, and 17.0% and 15.1% in canal waters, respectively. Conversely, HeS was the primary driver of DOM assembly, followed by homogenizing dispersal (HD). The relative importance of HeS for DOM assembly in natural waters was 85.4%, which was significantly larger than that in canal waters (69.3%). The relative importance of HD for canal DOM assembly was 29.4%, while the value was 14.6% for natural DOM assembly.

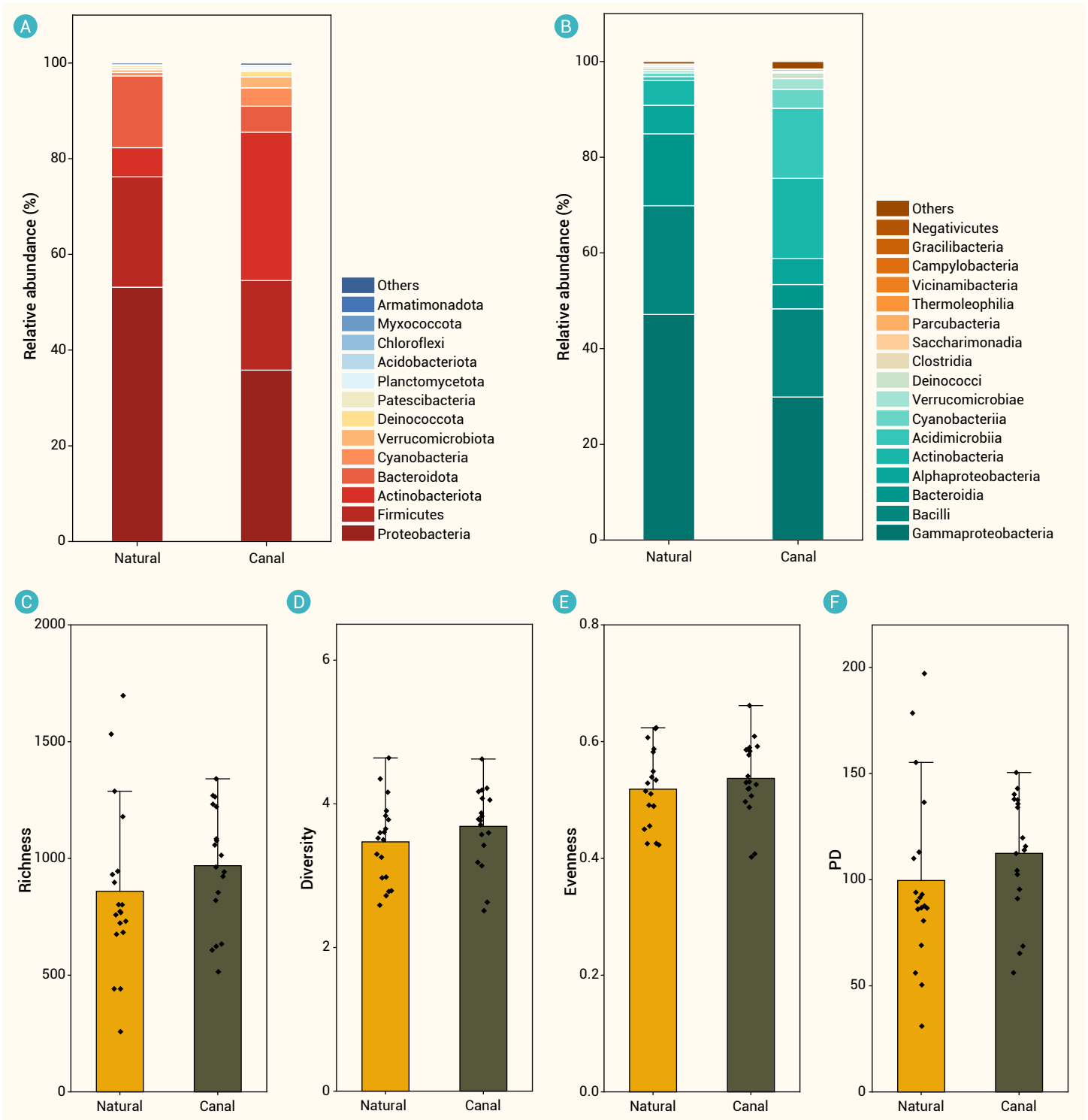

Figure 4. The bacterial communities in natural and canal waters (A) The bacterial community composition at the phylum level. (B) The bacterial community composition at the class level. (C) The community richness at ASV level. (D) The Shannon diversity at ASV level. (E) The Pielou's evenness at ASV level. (F) The Faith's phylogenetic diversity at ASV level.

Ecological networks between DOM and bacteria at a molecular level

To quantify the associations between DOM and bacteria, we first calculated the Spearman correlation coefficients (ρ) between each DOM molecule and bacterial ASV (Figure 7). According to potential resource-consumer relationships, negative and positive interactions may reflect microbial decomposition and production processes of organic matter, respectively.[33] Distinct DOM-microbe interaction patterns between canal and natural waters were observed. Canal DOM molecules were more likely to exhibit negative correlation with bacterial ASVs ($p < 0.05$), potentially reflecting microbial preference for or association with the transformation of larger or more complex molecules. Natural DOM generally showed a higher proportion of positive correlations ($p < 0.05$), indicating potential production of new molecules. Among the 1,861 DOM molecules involved in the canal DOM-microbe network, 567 molecules exhibited absolute positive correlations and 1,294 molecules showed absolute negative correlations with bacterial ASVs. In the natural DOM-microbe network, there were 1,921 DOM molecules, with 1,303 molecules showing absolute positive correlations and 618 molecules showing absolute negative correlations.

To further estimate the relationship between DOM molecules and microbial ASVs, we mapped the positive and negative correlation coefficients with

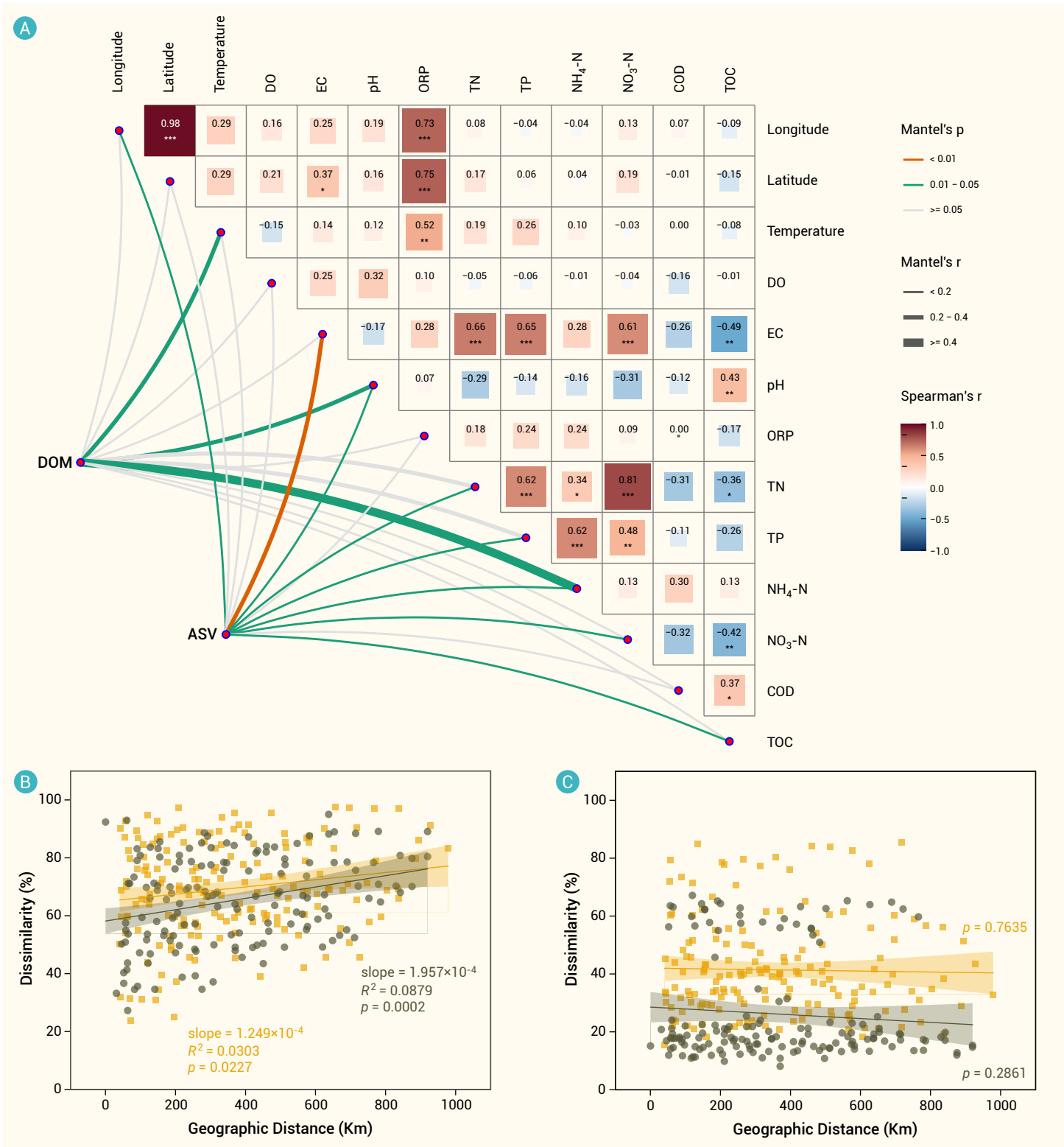

Figure 5. The relationship between environmental variables and DOM composition or bacterial community (A) Correlations of the DOM composition and microbial communities with the environmental variables. Edge width corresponds to the Mantel's r value, and the edge color denotes the statistical significance; pairwise correlations of the variables are shown with a color gradient denoting Pearson's correlation coefficients, asterisk shows the significance, * $p < 0.05$, ** $p < 0.01$, *** $p < 0.001$. (B) Distance-decay relationships based on Bray-Curtis dissimilarity of microbial communities in natural (yellow dot) and canal (dark square) waters. (C) Distance-decay relationships based on Bray-Curtis dissimilarity of DOM composition in natural (yellow dot) and canal (dark square) waters.

the rRNA gene operon (*rrn*) copy number of each ASV, which could reflect the growth rate and nutrient utilization efficiency of individual organisms.[48] The results clearly supported that the prevalence of positive ρ values was less than negative ρ values in canal waters, whereas the reverse pattern was observed in natural waters. The divergence between natural and canal waters was more significant for the ASVs with larger *rrn* copy numbers. As species with high *rrn* copy numbers are favored in copiotrophic environments, we may infer that the natural waters supplied a relative copiotrophic environment for microorganisms, whereas the canal waters were relatively oligotrophic. This result was also evidenced by the higher values of the community *rrn* copy number (Figure S5) in natural waters (mean 4.26) than those in canal waters (mean 3.17).

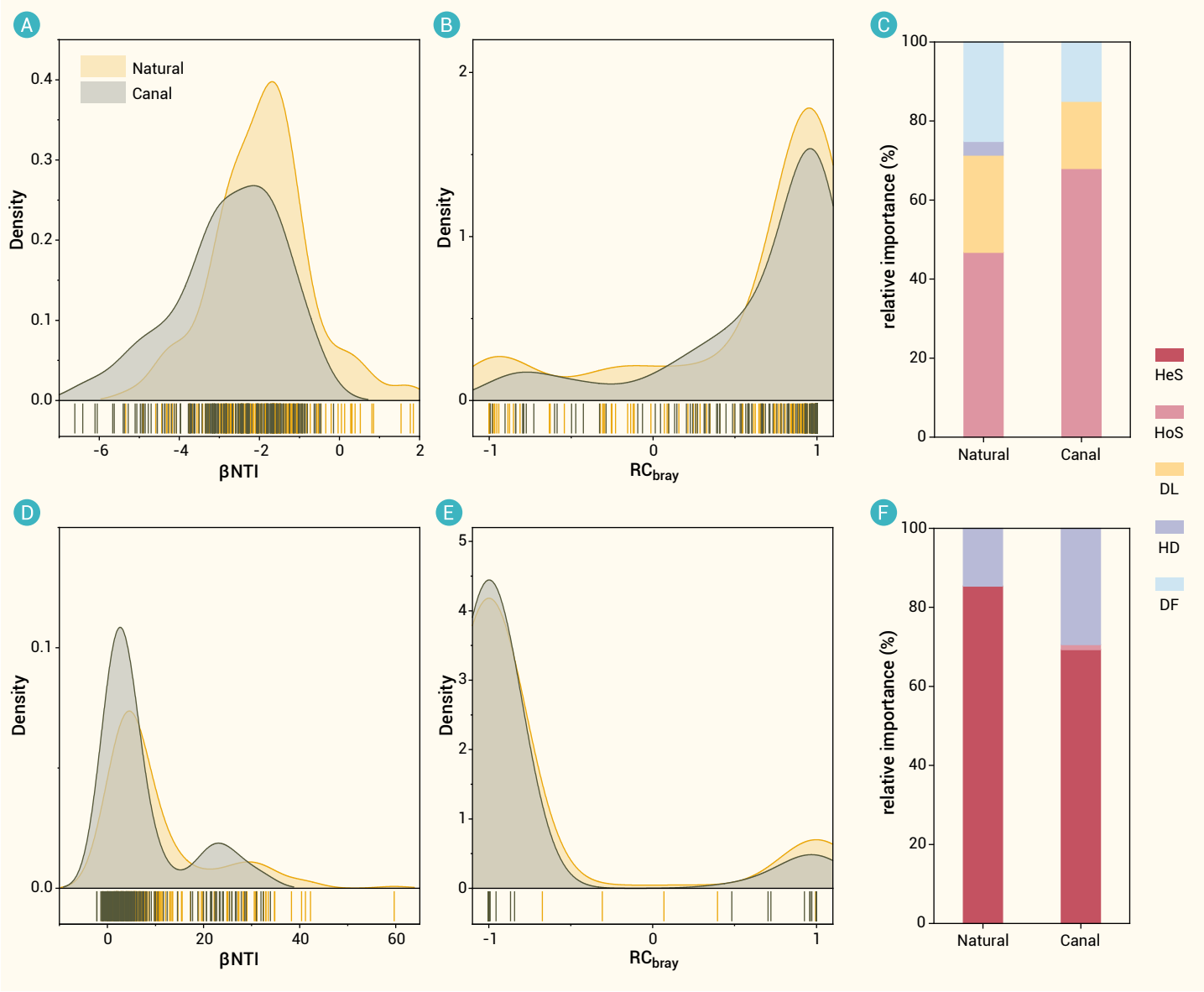

Figure 6. The null model results of microbial communities and DOM composition (A) Marginal density plots showing the distribution of standardized phylogenetic turnover of bacterial communities among natural and canal samples. (B) Marginal density plots showing the distribution of standardized taxonomic turnover of bacterial communities among natural and canal samples. (C) the relative importance of different ecological processes to the assembly of microbial community. (D) Marginal density plots showing the distribution of standardized dendrogram turnover of DOM composition among natural and canal samples. (E) Marginal density plots showing the distribution of standardized molecular turnover of DOM composition among natural and canal samples. (F) the relative importance of different ecological processes to the assembly of DOM composition. HeS, heterogeneous selection; HoS, homogeneous selection; HD, homogenizing dispersal; DL, dispersal limitation; DF, drift.

We subsequently quantified the DOM-ASV interactions using Sparse Correlations for Compositional data (SparCC), and found the interactions varied between the canal and natural waters. In canal waters, negative interactions were dominant between the molecules in lignin/tannins-like compounds and the bacteria in phyla Firmicutes, Alpha-Proteobacteria, or Gamma-Proteobacteria (Figure 8A), while the positive interactions involved Actinobacteriota or Firmicutes (Figure 8B). In natural waters, the molecules involved in the DOM-ASV interactions primarily belonged to the lignin-like or protein/amino sugar-like compounds, and the bacteria were mostly belonged to the phyla Alpha-Proteobacteria or Gamma-Proteobacteria (Figures 8C-D). Comparing the DOM-ASV interactions in natural and canal waters, we could observe that the Gamma-proteobacteria and Bacteroidota played more important roles in natural waters, whereas Firmicutes and Actinobacteriota showed more associations in canal waters. Gamma-proteobacteria and Bacteroidota are fast-growing copiotrophic organisms that can utilize labile organic substrates.[49] The Firmicutes and Actinobacteriota are endowed with numerous enzymes for depolymerization of more complex organic matter.[50,51] These findings align with the observed recalcitrance of canal DOM, suggesting lower bioavailability in this engineered system.

DISCUSSION

The observed increase in DOM recalcitrance within the canal waters, as evidenced by higher O/C, NOSC, and lower ΔG values, directly supports our hypothesis that the unique environment of the semi-enclosed concreted channel would promote the accumulation of more recalcitrant DOM. This is a crucial finding with significant impacts on carbon cycling and water quality.[52] The unshaded, open design of the canal exposes the water to intense solar radiation, which likely drives photochemical transformations of DOM. Additionally, the concrete lining of the canal creates a simplified ecosystem with limited exchange, leading to repeated photochemical and microbial metabolic transformations of DOM and the subsequent formation of refractory DOM.[53] The increased availability of oxygen in the well-mixed canal waters may also promote oxidative processes, further contributing to DOM recalcitrance through the formation of oxidized organic molecules.[54] Furthermore, the limited input of fresh allochthonous organic matter from riparian vegetation and sediments in the concreted canal contrasts with natural rivers, where a

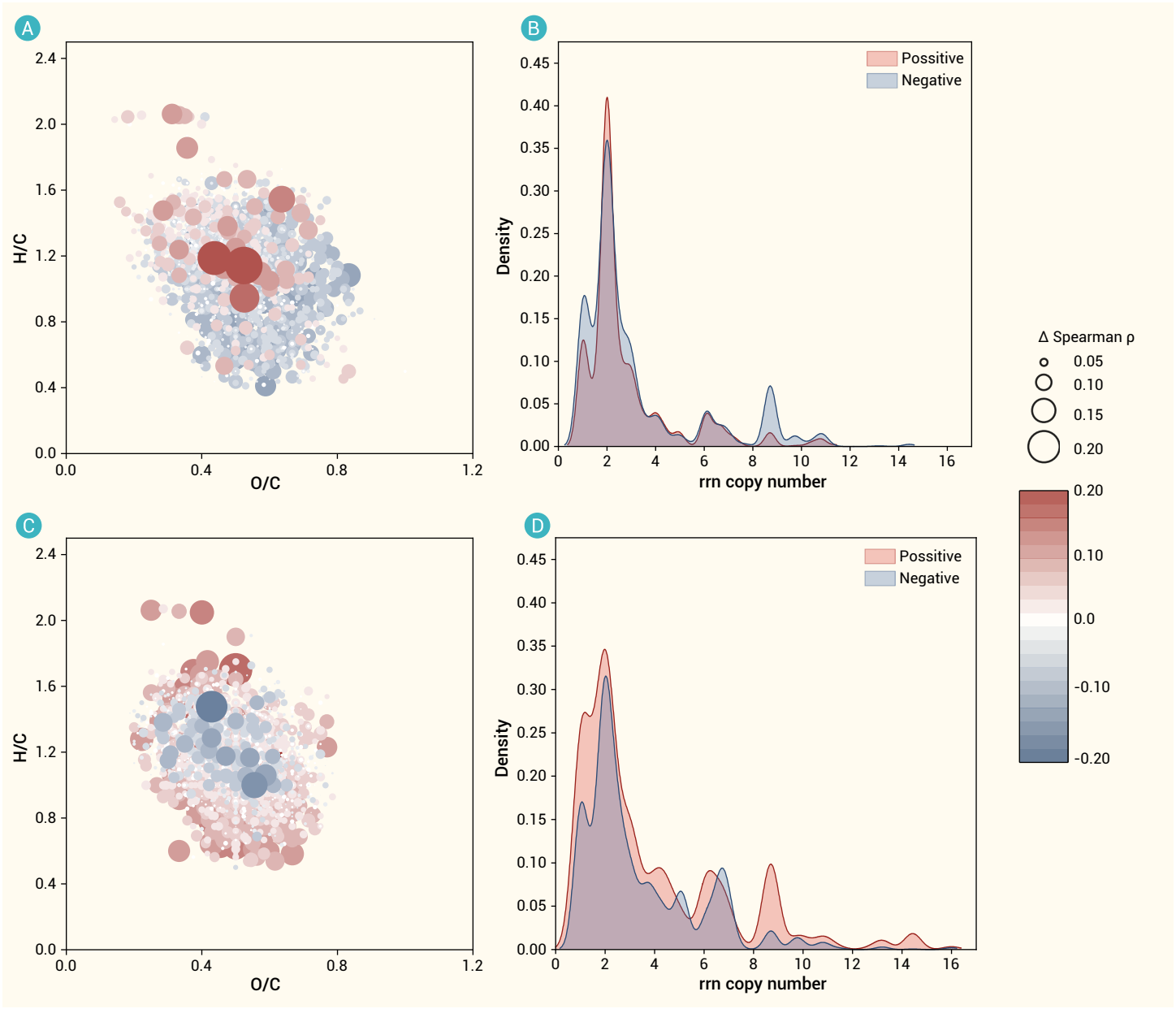

Figure 7. Association between DOM molecules and bacterial ASVs (A) Strength of the correlations between DOM molecules and bacterial ASVs in canal waters. (B) Strength of the correlations between DOM molecules and bacterial ASVs in natural waters. For each molecule across all samples in each treatment, we subtracted the mean absolute Spearman's rank correlation coefficient ρ of all the negative correlations with individual bacterial ASVs from the mean of the positive correlations to derive Δρ. Δρ was further visualized against the molecular H/C and O/C. (C) Marginal density plots showing the negative and position correlation between DOM molecules and bacterial ASVs along the rRNA gene operon (*rrn*) copy number in canal waters. (D) Marginal density plots showing the negative and position correlation between DOM molecules and bacterial ASVs along the rRNA gene operon (*rrn*) copy number in natural waters.

continuous supply of labile organic matter from terrestrial sources can dilute the pool of recalcitrant DOM. The absence of this input in the canal likely leads to a relative enrichment of aged, processed DOM. This shift towards more recalcitrant DOM might also contribute to the observed greater homogeneity of DOM canal waters, as the continuous processing might lead to a more uniform pool of these compounds. The lower ΔG values in canal DOM suggest that the molecular transformations are less thermodynamically favorable, indicating higher stability and lower reactivity of the DOM molecules.[35] The DOM recalcitrance in the canal waters is also reflected by the greater relative abundance of Actinobacteriota. Studies have shown that Actinobacteriota possess a diverse array of enzymes enabling then to preferentially metabolize structurally complex and recalcitrant DOM components, such as lignin-derived compounds, indicating their potential specialization in sustaining carbon turnover under low-nutrient conditions.[13,50,51] This accumulation of recalcitrant DOM in the canal may have significant implications for the long-term management of the SNWD project and the quality of the water it delivers. Recalcitrant DOM is less readily utilized by microorganisms, potentially leading to a lower rate of microbial respiration and a slower turnover of organic carbon.[55] The persistent DOM can also affect the availability of light and nutrients for other aquatic organisms.[55,56] Moreover, the long-term accumulation of recalcitrant DOM may contribute to the formation of disinfection by-products during water treatment processes, potentially requiring adjustments to treatment strategies.[52]

Our findings revealed a notable homogeneity in both DOM molecular composition and microbial community structure within the canal waters compared to the natural river systems. This pattern suggests that the canal environment, as an engineered system with a more stable and less variable flow regime, exerts a strong selective pressure, leading to a convergence of ecological characteristics such as the types of DOM molecues and the dominant microbial taxa.[57] Several factors could contribute to this homogenization. Firstly, the consistent, controlled flow regime within the canal, as opposed to the more fluctuating hydrological conditions of natural rivers,

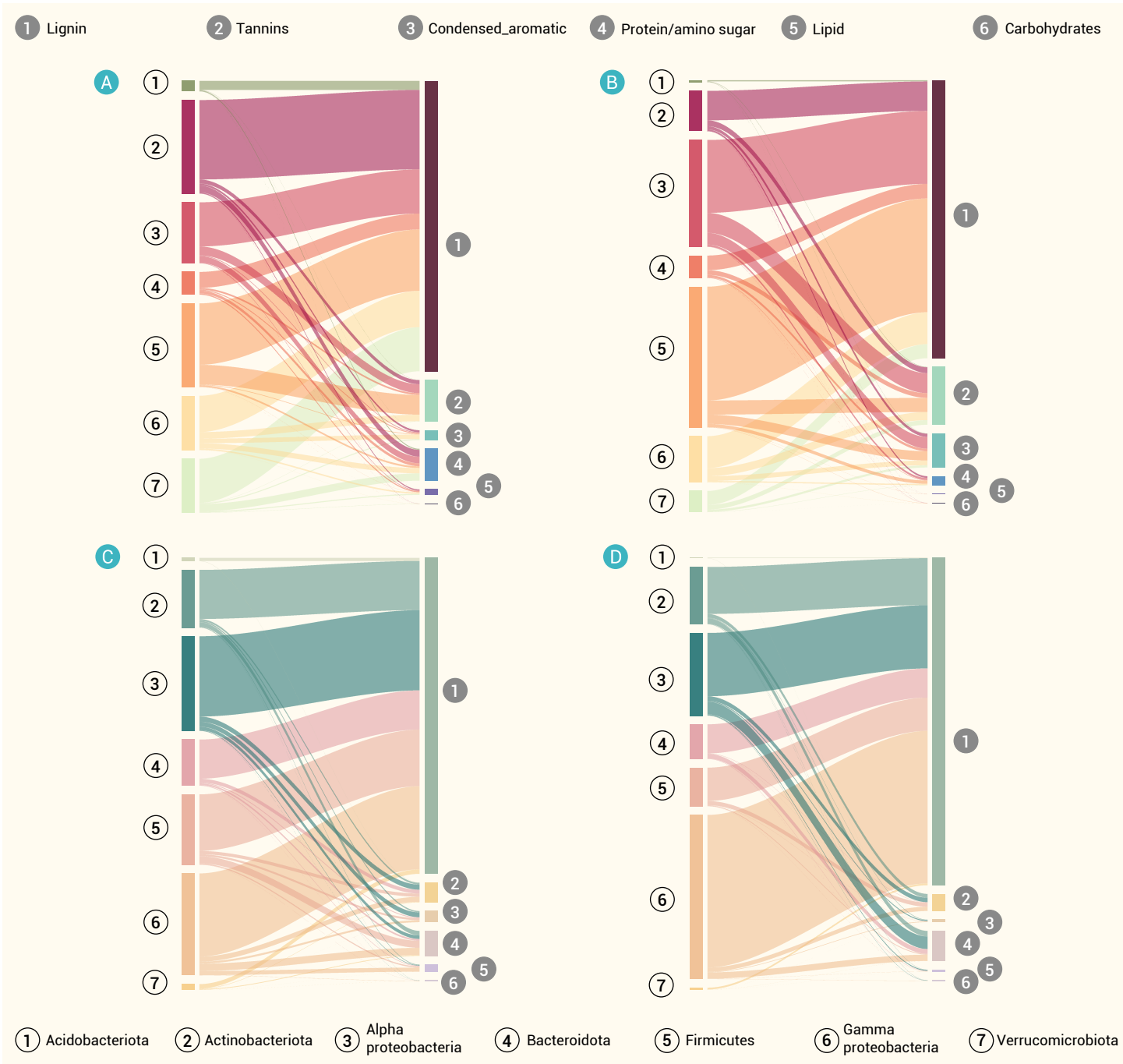

Figure 8. Bipartite networks between DOM molecules and bacterial ASVs colored by the phylum (A) Negative bipartite network between DOM molecules and bacterial ASVs in canal waters estimated using SparCC. (B) Positive bipartite network between DOM molecules and bacterial ASVs in canal waters estimated using SparCC. (C) Negative bipartite network between DOM molecules and bacterial ASVs in natural waters estimated using SparCC. (D) Positive bipartite network between DOM molecules and bacterial ASVs in natural waters estimated using SparCC.

reduced environmental heterogeneity.[58] This changeless environment may favor a specific subset of microbial taxa and DOM molecules that are adapted to these consistent conditions, leading to a reduction in overall diversity and an increase in similarity across sampling sites.[58] Secondly, the concrete lining of the canal, which eliminates interactions with natural sediments and riparian vegetation, may further homogenize the aquatic environment. The absence of diverse allochthonous inputs and the reduction of natural biogeochemical processes likely contribute to a more uniform DOM composition and microbial community. In this enclosed ecosystem, DOM may undergo repeated microbial and photochemical degradation, gradually converging toward more similar properties along the canal's course. The higher homogeneity of microbial communities in the canal may also reflect the selective pressure of the canal's physical and chemical conditions.[57] For instance, the consistent sunlight exposure and potential for increased photooxidation may select for specific phototolerant microbial taxa, as evidenced by the higher abundance of Cyanobacteria in canal waters.[59] Furthermore, the relative limited nutrient variability and the consistent water source from the Danjiangkou Reservoir may also contribute to a more uniform microbial community composition throughout the canal system.

Even though homogeneity in both DOM molecular composition and microbial community structure was observed, the underlying ecological mechanisms were different. The null model revealed that the homogeneity in DOM was attributed to the reduced heterogeneous selection and the increased homogenizing dispersal, whereas homogeneous selection governed the microbial assembly in canal waters and induced the homogeneity.[42] Homogenizing dispersal is generally driven by the physical movement, such as the

consistent water flow in the canal, while homogeneous selection refers to the process where similar environmental conditions across different habitats select for similar microbial communities. Our findings suggest that homogeneity in DOM molecules was primarily due to the consistent flow regime in canal waters. Additionally, our findings suggested that environmental variables play more significant roles in shaping microbial communities than the DOM compositions. Thus, the DOM homogeneity may also be a consequence of the microbial transformation.

This observed homogenization may have important implications for ecosystem functioning. Modifications to within- and between-community trait composition will probably impinge upon community and ecosystem function, and resistance to environmental change. A decrease in community diversity may reduce overall community and ecosystem functioning, stability and resistance to environmental perturbations by simply narrowing the available range of species-specific responses.[46,57–59] Thus, the more homogeneous microbial assemblages in the canal water may exhibit lower functional redundancy, limiting its capacity to buffer against abrupt changes in nutrient availability or contaminant inputs. Additionally, the reduced diversity of DOM molecules may limit the range of microbial metabolic pathways and potentially affect the overall carbon cycling within the canal or the receiving waters.[60] Furthermore, distinct microbe-DOM interaction networks were observed between canal and natural waters, with canal ecosystems exhibiting a higher prevalence of competitive microbial relationships. This finding potentially suggested microbial decomposition processes may dominate over organic matter production within the canal system, likely driven by the optimal conditions for photo-mineralization in the unshaded canal. Whether this process would influence CO_2 emissions from canal waters should be evaluated by integrating *in situ* monitoring with controlled light-exposure and microbial incubation experiments in further studies.

Taken together, the eco-environmental trade-offs of water diversion require careful consideration in the SNWD project.[61] If water transfer infrastructure is proven to elevate carbon emissions, policy-makers should reconcile the environmental ramifications of water diversion with the fulfillment of water demand. It is recommended to implement dynamic control systems to optimize water flow rates and strategically enhance nighttime water transfers, Furthermore, it is imperative to urgently prioritize the sustainable infrastructure designs, such as underground pipelines, to mitigate the exacerbating effects of climate change, which still requires scientific verification. Additionally, pollution reduction measures should be introduced at critical nodes along the transfer route. More broadly, Integrating the carbon reduction strategies and technologies into the future construction of national water network represents a critical advancement towards ensuring sustainable water resources management in the face of increasing environmental pressures.

REFERENCES

1. Battin T. J., Luyssaert S., Kaplan L. A., et al. (2009). The boundless carbon cycle. *Nat. Geosci.* **2**:598–600. DOI:10.1038/ngeo618
2. Lapierre J. F., Guillemette F., Berggren M., et al. (2013). Increases in terrestrially derived carbon stimulate organic carbon processing and CO_2 emissions in boreal aquatic ecosystems. *Nat. Commun.* **4**:2972. DOI:10.1038/ncomms3972
3. Catalá T. S., Reche I., Fuentes-Lema A., et al. (2015). Turnover time of fluorescent dissolved organic matter in the dark global ocean. *Nat. Commun.* **6**:5986. DOI:10.1038/ncomms6986
4. Monteith D. T., Stoddard J. L., Evans C. D., et al. (2007). Dissolved organic carbon trends resulting from changes in atmospheric deposition chemistry. *Nature* **450**:537–540. DOI:10.1038/nature06316
5. Tanentzap A. J., Fitch A., Orland C., et al. (2019). Chemical and microbial diversity covary in fresh water to influence ecosystem functioning. *Proc. Natl. Acad. Sci. USA* **116**:24689–24695. DOI:10.1073/pnas.1904896116
6. Tanentzap A. J. and Fonvielle J. A. (2024). Chemodiversity in freshwater health. *Science* **383**:1412–1414. DOI:10.1126/science.adg8658
7. Dittmar T., Lennartz S. T., Buck-Wiese H., et al. (2021). Enigmatic persistence of dissolved organic matter in the ocean. *Nat. Rev. Earth Env.* **2**:570–583. DOI:10.1038/s43017-021-00183-7
8. Hu A., Jang K. S., Tanentzap A. J., et al. (2024). Thermal responses of dissolved organic matter under global change. *Nat. Commun.* **15**:576. DOI:10.1038/s41467-024-44813-2
9. Osterholz H., Singer G., Wemheuer B., et al. (2016). Deciphering associations between dissolved organic molecules and bacterial communities in a pelagic marine system. *ISME J.* **10**:1717–1730. DOI:10.1038/ismej.2015.231
10. Zhou L., Zhou Y., Tang X., et al. (2021). Resource aromaticity affects bacterial community successions in response to different sources of dissolved organic matter. *Water Res.* **190**:116776. DOI:10.1016/j.watres.2020.116776
11. Jiao N., Luo T., Chen Q., et al. (2024). The microbial carbon pump and climate change. *Nat. Rev. Microbiol.* **22**:408–419. DOI:10.1038/s41579-024-01018-0
12. McDonough L. K., Andersen M. S., Behnke M. I., et al. (2022). A new conceptual framework for the transformation of groundwater dissolved organic matter. *Nat. Commun.* **13**:2153. DOI:10.1038/s41467-022-29711-9
13. Wang K., Pang Y., Yi Y., et al. (2023). Response of dissolved organic matter chemistry to flood control of a large river reservoir during an extreme storm event. *Water Res.* **230**:119565. DOI:10.1016/j.watres.2023.119565
14. He J., Yang Y., Wu X., et al. (2022). Responses of dissolved organic matter (DOM) characteristics in eutrophic lake to water diversion from external watershed. *Environ. Pollut.* **312**:119992. DOI:10.1016/j.envpol.2022.119992
15. Zhou Y., Chen L., Zhou L., et al. (2023). Key factors driving dissolved organic matter composition and bioavailability in lakes situated along the eastern route of the South-to-North water diversion project, China. *Water Res.* **233**:119782. DOI:10.1016/j.watres.2023.119782
16. Wilson H. F., Xenopoulos M. A., Wilson H. F., et al. (2008). Effects of agricultural land use on the composition of fluvial dissolved organic matter. *Nat. Geosci.* **2**:37–41. DOI:10.1038/ngeo391
17. Zeng X., Zheng Y., Chen X., et al. (2023). Molecular responses of dissolved organic matter to anthropogenic groundwater recharge: Characteristics, transformations, and sensitive molecules. *Environ. Sci. Technol.* **57**:7789–7799. DOI:10.1021/acs.est.2c08353
18. Zheng Y., He W., Li B., et al. (2020). Refractory humic-like dubstances: Tracking rnvironmental impacts of anthropogenic groundwater Recharge. *Environ. Sci. Technol.* **54**:15778–15788. DOI:10.1021/acs.est.0c04561
19. Herzsprung P., von Tumpling W., Hertkorn N., et al. (2012). Variations of DOM quality in inflows of a drinking water reservoir: Linking of van Krevelen diagrams with EEMF spectra by rank correlation. *Environ. Sci. Technol.* **46**:5511–5518. DOI:10.1021/es300345c
20. Siddik M. A. B., Dickson K. E., Rising J., et al. (2023). Interbasin water transfers in the United States and Canada. *Sci. Data* **10**:27. DOI:10.1038/s41597-023-01935-4
21. Liu N., Dobbs G. R., Caldwell P. V., et al. (2022). Inter - Basin tansfers extend the benefits of eater from forests to population venters across the conterminous U. S. *Water Resour. Res.* **58**:e2021WR031537. DOI:10.1029/2021WR031537
22. Sheng J., Zhang R. and Yang H. (2024). Inter-basin water transfers and water rebound effects: The South-North water transfer project in China. *J. Hydrol.* **638**:131516. DOI:10.1016/j.jhydrol.2024.131516
23. Bowen J. C., Wahyudio P. J., Anshari G. Z., et al. (2024). Canal networks regulate aquatic losses of carbon from degraded tropical peatlands. *Nat. Geosci.* **17**:213–218. DOI:10.1038/s41561-024-01383-8
24. Hou C., Chen L., Dong Y., et al. (2022). Unraveling dissolved organic matter in drinking water through integrated ozonation/ceramic membrane and biological activated carbon process using FT-ICR MS. *Water Res.* **222**:118881. DOI:10.1016/j.watres.2022.118881
25. Xu W., Gao Q., He C., et al. (2020). Using ESI FT-ICR MS to characterize dissolved organic matter in salt lakes with different salinity. *Environ. Sci. Technol.* **54**:12929–12937. DOI:10.1021/acs.est.0c01681
26. Dittmar T., Koch B., Hertkorn N., et al. (2008). A simple and efficient method for the solid - phase extraction of dissolved organic matter (SPE - DOM) from seawater. *Limnol. Oceanogr. Meth.* **6**:230–235. DOI:10.4319/lom.2008.6.230
27. Sun Y., Li X., Li X., et al. (2022). Deciphering the fingerprint of dissolved organic matter in the soil amended with biodegradable and conventional microplastics based on optical and molecular signatures. *Environ. Sci. Technol.* **56**:15746–15759. DOI:10.1021/acs.est.2c06258
28. Corilo Y. E., Kew W. R. and McCue L. A. EMSL-Computing/CoreMS: CoreMS 3.0.0. DOI:10.5281/zenodo.4641552
29. Kujawinski E. B. and Behn M. D. (2006). Automated analysis of electrospray ionization fourier transform ion cyclotron resonance mass spectra of natural organic matter. *Anal. Chem.* **78**:4363–4373. DOI:10.1021/ac0600306
30. D'Andrilli J., Cooper W. T., Foreman C. M., et al. (2015). An ultrahigh-resolution mass spectrometry index to estimate natural organic matter lability. *Rapid Commun. Mass Spectrom.* **29**:2385–2401. DOI:10.1002/rcm.7400
31. Hughey C. A., Hendrickson C. L., Rodgers R. P., et al. (2001). Kendrick mass defect spectrum: A compact visual analysis for Ultrahigh-Resolution broadband mass spectra. *Anal. Chem.* **73**:4676–4681. DOI:10.1021/ac010560w
32. Song H. S., Stegen J. C., Graham E. B., et al. (2020). Representing organic matter thermodynamics in biogeochemical reactions via substrate-explicit modeling. *Front. Microbiol.* **11**:531756. DOI:10.3389/fmicb.2020.531756
33. Hu A., Choi M., Tanentzap A. J., et al. (2022). Ecological networks of dissolved organic matter and microorganisms under global change. *Nat. Commun.* **13**:3600. DOI:10.1038/s41467-022-31251-1
34. Wu M., Li P., Li G., et al. (2022). Using potential molecular transformation to understand the molecular trade-offs in soil dissolved organic matter. *Environ. Sci. Technol.* **56**:11827–11834. DOI:10.1021/acs.est.2c01137

35. LaRowe D. E. and Cappellen P. V. (2011). Degradation of natural organic matter: A thermodynamic analysis. *Geochim. Cosmochim. Acta* **75**:2030–2042. DOI:10.1016/j.gca.2011.01.020
36. Callahan B. J., McMurdie P. J., Rosen M. J., et al. (2016). DADA2: High-resolution sample inference from Illumina amplicon data. *Nat. Methods* **13**:581–583. DOI:10.1038/nmeth.3869
37. Quast C., Pruesse E., Yilmaz P., et al. (2013). The SILVA ribosomal RNA gene database project: Improved data processing and web-based tools. *Nucleic Acids Res.* **41**:D590–596. DOI:10.1093/nar/gks1219
38. Anderson M. J. and Walsh D. C. I. (2013). PERMANOVA, ANOSIM, and the Mantel test in the face of heterogeneous dispersions: What null hypothesis are you testing. *Ecol. Monogr.* **83**:557–574. DOI:10.1890/12-2010.1
39. Webb C. O., Ackerly D. D., McPeek M. A., et al. (2002). Phylogenies and community ecology. *Annu. Rev. Ecol. Evol. S.* **33**:475–505. DOI:10.1146/annurev.ecolsys.33.010802.150448
40. Danczak R. E., Chu R. K., Fansler S. J., et al. (2020). Using metacommunity ecology to understand environmental metabolomes. *Nat. Commun.* **11**:6369. DOI:10.1038/s41467-020-19989-y
41. She Z., Wang J., Wang S., et al. (2023). Quantifying stochastic processes in shaping dissolved organic matter pool with high-tesolution mass spectrometry. *Environ. Sci. Technol.* **57**:16361–16371. DOI:10.1021/acs.est.3c07046
42. Stegen J. C., Lin X., Fredrickson J. K., et al. (2013). Quantifying community assembly processes and identifying features that impose them. *ISME J.* **7**:2069–2079. DOI:10.1038/ismej.2013.93
43. Ning D., Yuan M., Wu L., et al. (2020). A quantitative framework reveals ecological drivers of grassland microbial community assembly in response to warming. *Nat. Commun.* **11**:4717. DOI:10.1038/s41467-020-18560-z
44. Peres-Neto P. R. and Jackson D. A. (2001). How well do multivariate data sets match. The advantages of a Procrustean superimposition approach over the Mantel test. *Oecologia* **129**:169–178. DOI:10.1007/s004420100720
45. Legendre P. and Fortin M. J. (2010). Comparison of the Mantel test and alternative approaches for detecting complex multivariate relationships in the spatial analysis of genetic data. *Mol. Ecol. Resour.* **10**:831–844. DOI:10.1111/j.1755-0998.2010.02866.x
46. Allison S. D. and Martiny J. B. (2008). Colloquium paper: Resistance, resilience, and redundancy in microbial communities. *Proc. Natl. Acad. Sci. USA* **105 Suppl 1**:11512-11519. DOI:10.1073/pnas.0801925105
47. Friedman J. and Alm E. J. (2012). Inferring correlation networks from genomic survey data. *PLOS Comput. Biol.* **8**:e1002687. DOI:10.1371/journal.pcbi.1002687
48. Roller B. R., Stoddard S. F. and Schmidt T. M. (2016). Exploiting rRNA operon copy number to investigate bacterial reproductive strategies. *Nat. Microbiol.* **1**:16160. DOI:10.1038/nmicrobiol.2016.160
49. Ling N., Wang T. and Kuzyakov Y. (2022). Rhizosphere bacteriome structure and functions. *Nat. Commun.* **13**:836. DOI:10.1038/s41467-022-28448-9
50. Huang J., Gao K., Yang L., et al. (2023). Successional action of Bacteroidota and Firmicutes in decomposing straw polymers in a paddy soil. *Environ. Microbiome* **18**:76. DOI:10.1186/s40793-023-00533-6
51. Nweze J. E., Sustr V., Brune A., et al. (2024). Functional similarity, despite taxonomical divergence in the millipede gut microbiota, points to a common trophic strategy. *Microbiome* **12**:16. DOI:10.1186/s40168-023-01731-7
52. Berg S. M., Wammer K. H. and Remucal C. K. (2023). Dissolved organic matter photoreactivity is determined by its optical properties, redox activity, and molecular composition. *Environ. Sci. Technol.* **57**:6703–6711. DOI:10.1021/acs.est.3c01157
53. An S., Du Y., Huang X., et al. (2024). Long-term photochemical and microbial alterations lead to the compositional convergence of algal and terrestrial dissolved organic matter. *Environ. Sci. Technol.* **58**:18765–18776. DOI:10.1021/acs.est.4c07307
54. Chen X., Liu J., Chen J., et al. (2022). Oxygen availability driven trends in DOM molecular composition and reactivity in a seasonally stratified fjord. *Water Res.* **220**:118690. DOI:10.1016/j.watres.2022.118690
55. Yang X., Zhang S., Wu D., et al. (2024). Recalcitrant components accumulation in dissolved organic matter decreases microbial metabolic quotient of red soil under long-term manuring. *Sci. Total Environ.* **934**:173287. DOI:10.1016/j.scitotenv.2024.173287
56. Logue J. B., Stedmon C. A., Kellerman A. M., et al. (2016). Experimental insights into the importance of aquatic bacterial community composition to the degradation of dissolved organic matter. *ISME J.* **10**:533–545. DOI:10.1038/ismej.2015.131
57. Ning D., Wang Y., Fan Y., et al. (2024). Environmental stress mediates groundwater microbial community assembly. *Nat. Microbiol.* **9**:490–501. DOI:10.1038/s41564-023-01573-x
58. Stegen J. C., Lin X., Konopka A. E., et al. (2012). Stochastic and deterministic assembly processes in subsurface microbial communities. *ISME J.* **6**:1653–1664. DOI:10.1038/ismej.2012.22
59. Louca S., Polz M. F., Mazel F., et al. (2018). Function and functional redundancy in microbial systems. *Nat. Ecol. Evol.* **2**:936–943. DOI:10.1038/s41559-018-0519-1
60. Kujawinski E. B. (2011). The impact of microbial metabolism on marine dissolved organic matter. *Ann. Rev. Mari. Sci.* **3**:567–599. DOI:10.1146/annurev-marine-120308-081003
61. Yan H., Lin Y., Chen Q., et al. (2023). A review of the eco-environmental impacts of the South-to-North water diversion: Implications for interbasin water transfers. *Engineering* **30**:161–169. DOI:10.1016/j.eng.2023.05.012

FUNDING AND ACKNOWLEDGMENTS

This research was supported by the Beijing Natural Science Foundation (No. 5242011). The funders had no role in study design, data collection and analysis, decision to publish, or preparation of the manuscript.

AUTHOR CONTRIBUTIONS

X.F.C. and J.W. conceived and performed the study. Z.T.S., J.H.J. and Y.W.W. collected and analyzed the data. X.F.C. and J.W. led the analysis and writing. J.Y.C., W.X.Q., J.F.P., H.J.L. and J.H.Q. contributed to the revision. H.J.L. and J.H.Q. supervised the manuscript. All authors contributed to the manuscript and approved the final version.

DECLARATION OF INTERESTS

The authors declare no competing interests.

DATA AND CODE AVAILABILITY

Data are available from the corresponding author upon reasonable request.

SUPPLEMENTAL INFORMATION

It can be found online at https://doi.org/10.59717/j.xinn-geo.2025.100170